



EXAFS studies of catalytic DNA sensors for mercury contamination of water

B. Ravel^{a,*}, S.C. Slimmer^b, X. Meng^c, G.C.L. Wong^{b,d}, Y. Lu^{b,c}^a National Institute of Standards and Technology, 100 Bureau Drive, Gaithersburg, MD 20899, United States, United States^b Department of Materials Science and Engineering, University of Illinois at Urbana-Champaign, 1304 West Green Street, Urbana, IL 61801, United States^c Department of Chemistry, University of Illinois at Urbana-Champaign, Urbana, IL 61801, United States^d Departments of Physics and Bioengineering, University of Illinois at Urbana-Champaign, Urbana, IL 61801, United States

ARTICLE INFO

Keywords:

EXAFS
DNA
Sensor
Mercury
Contamination

ABSTRACT

Monitoring of metallic contaminants in domestic and agricultural water systems requires technology that is fast, flexible, sensitive, and selective. Recently, metal sensors based on catalytic DNA have been demonstrated as a practical monitoring solution. Very little is known, however, about the atomic scale interactions between the DNA-based sensors and the metal contaminant to which the sensor is targeted. Here, we present the results of an X-ray absorption spectroscopy study of a mercury sensor which illustrates the nature of the Hg–DNA interaction.

Published by Elsevier Ltd.

1. Introduction

Water systems used for domestic and agricultural applications can be adversely affected by toxic, heavy metal contaminants through human activities such as mining and industrial production as well as by contact with natural reservoirs of those metals. Safe use of these water supplies requires timely monitoring of bioavailable metallic species, followed by remediation in the event of contamination. A useful monitoring technology must be fast, flexible, sensitive, and selective. The criterion of speed requires that results can be obtained immediately and in the field setting. This technology must be easily transported to and deployed in the location of the contaminated water. It must detect levels of contamination at or below regulated human health levels. Finally, the technology must be selective in the sense of responding positively only to the targeted element.

Recently, catalytic DNA sensors meeting all of these criteria have been developed (Li and Lu, 2000; Liu and Lu, 2007; Liu et al., 2007). High selectivity is obtained by an active DNA sequence showing a very high affinity for a target metal species. The binding of the target metal to this site cleaves the DNA, separating a fluorophore from a quencher, both of which are bound to ends of the DNA strand. This is shown schematically in Fig. 1. Once separated, the fluorophore releases a photon which can be detected via a photodiode. Sensitivities below 100 µg/kg have been demonstrated along with as high as million-fold levels of selectivity.

Although the performance of the sensor is well-demonstrated, the atomic interaction between the metallic contaminant and the

catalytic DNA is not well understood. In this paper, we present the results of extended X-ray-absorption spectroscopy (EXAFS) measurements on a 10 base-pair, double-stranded DNA duplex that contains the same mercury binding site as the larger catalytic DNA sensor for mercury. One purpose of this paper is to examine the nature of the metal/DNA binding on the atomic scale. Because these are proceedings of a synchrotron summer school, the second purpose of this work is to demonstrate an advanced technique of EXAFS data analysis using the computer codes FEFF (Rehr and Albers, 2000) and IFEFFIT (Newville, 2001).

2. Sample preparation

Three distinct Hg-containing samples were prepared using mercury(II) perchlorate and a 10 base pair double-stranded DNA duplex (5′–CGCGTTGTCC–3′: 5′–GGACTTCGCG–3′) that has been previously reported to contain two Hg binding sites, one at each of the two consecutive T–T mispairs (Miyake et al., 2006; Tanaka et al., 2006, 2007). The DNA duplex was synthesized commercially as two single-stranded DNA oligomers by Integrated DNA Technologies (Coralville, IA).¹

The first sample contained 3 mM Hg(II) and 3 mM duplex DNA, thus yielding a 1:2 ratio of Hg(II) ions to T–T mispairs. The second sample contained 6 mM Hg(II) and 3 mM duplex DNA, thus yielding a 1:1 ratio of Hg(II) ions to T–T mispairs. The control sample contained 15 mM Hg(II) and 0 mM duplex DNA. All three

* Corresponding author.

E-mail address: bruce.ravel@nist.gov (B. Ravel).

¹ Certain commercial equipment, instruments, or materials are identified in this article in order to specify the experimental procedure adequately. Such identification is not intended to imply recommendation or endorsement by the National Institute of Standards and Technology, nor is it intended to imply that the materials or equipment are necessarily the best available for this purpose.

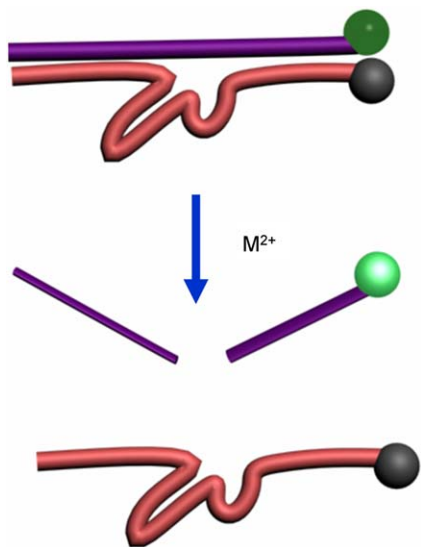


Fig. 1. Schematic representation of interaction of the DNA sensor and the target metal. The intact DNA duplex, shown in the top portion of the figure, comes in contact with its target metal ion M , in this case a Hg^{2+} ion. The binding site is cleaved, separating the fluorophore (green circle) bound to one strand from the quencher (gray circle) bound to the other strand. Once cleaved, the fluorophore releases a photon which can be detected easily. (For interpretation of the references to colour in this figure legend, the reader is referred to the web version of this article.)

samples were prepared in a pH 6.10 buffer containing 100 mM sodium perchlorate (to ensure proper ionic conditions), 50 mM sodium cacodylate (to control pH), and 20% glycerol (to aid in glassing when frozen).

3. EXAFS measurements

The solutions described above were pipetted into quartz capillary tubes (Charles Supper Company, Natick, MA) with an outer diameter of 1.5 mm and a wall thickness of 10 μ m. The quartz capillary tubes were flame sealed and doubly enclosed with small Kapton bags to provide containment in the case of a spill. Samples were then flash frozen in liquid nitrogen. The bagged capillaries were mounted onto a probe and placed into a Displex two-stage helium cryostat. A small pressure of helium was maintained in the sample volume as a heat exchange medium between the sample and the cold stabilizing the sample temperature around 10 K. The cold temperature was used to inhibit redox chemistry of the sample under the intense X-ray beam. All measurements were made at beamline 20BM at the Advanced Photon Source. A double-crystal Si(111) monochromator was detuned about 30% which, along with a flat mirror, was used to suppress harmonic content. A nitrogen-filled ionization chamber was used to measure the incident flux and the EXAFS was measured in the fluorescence geometry using a 13 element germanium detector. The beam was apertured to 1 mm by 1 mm and centered on the sample.

For each sample presented herein, multiple scans were measured and averaged. Data processing was accomplished using the ATHENA program (Ravel and Newville, 2005). Depending on the concentration of Hg in the sample, between 5 and 42 scans were averaged. Analysis of the EXAFS spectra, described in detail below, was accomplished using IFEFFIT and an unpublished programming interface (Ravel, 2008) under development by one of the authors.

4. Mercury sensors

EXAFS data were measured on the mercury sample with 3 mM each of Hg and DNA and on the Hg control sample. These data are shown in Fig. 2 and demonstrate a distinct difference in bonding environment for Hg in the presence of the DNA. Earlier nuclear magnetic resonance (NMR) studies (Miyake et al., 2006; Tanaka et al., 2006, 2007) on similar Hg-selective DNA compounds suggest that each T–T mismatch is a binding sites for the Hg. This possibility is easily tested using the sample prepared with excess Hg. Shown in Fig. 3 are data obtained on the sample containing 6 mM Hg along with 3 mM duplex DNA. If the DNA duplexes do offer two binding sites, then we expect the sample with 6 mM Hg to be substantively the same as the 3 mM Hg samples. Using linear combination analysis (Ravel and Newville, 2005), we find the 6 mM Hg sample to be well described by 54(1)% of the control and 46(1)% of the 3 mM Hg sample.

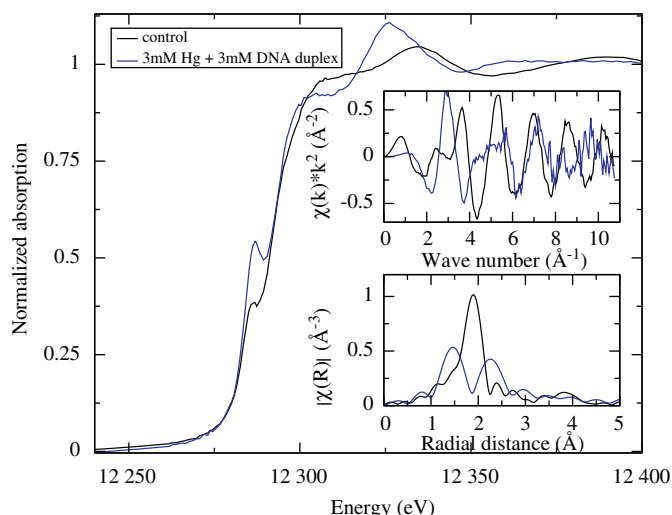


Fig. 2. EXAFS data measured on the Hg control (black) and the sample with 3 mM of Hg and 3 mM duplex DNA (blue). Substantial differences between the data, as seen in the normalized $\mu(E)$ spectrum as well as the $\chi(k)$ and $\chi(R)$ shown in the insets, demonstrate a bonding environment for the Hg in the presence of DNA which is distinct from the aqueous phase. (For interpretation of the references to colour in this figure legend, the reader is referred to the web version of this article.)

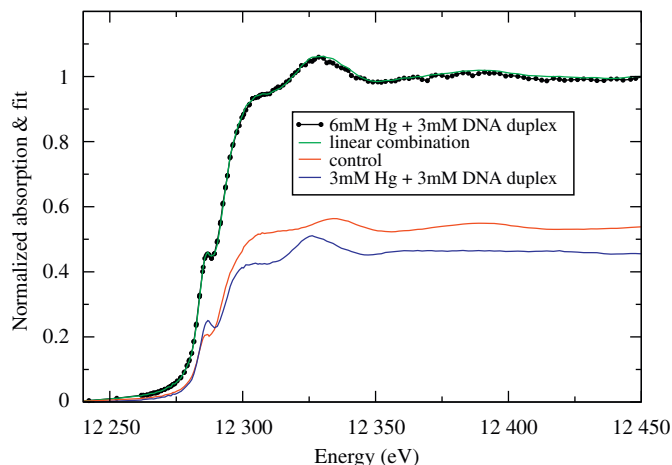


Fig. 3. Results of linear combination analysis of the data with excess Hg. The data (circles) are plotted with the fit (green). Also shown are the control (red) and 3 mM Hg (blue) samples scaled by 0.54 and 0.46, respectively. (For interpretation of the references to colour in this figure legend, the reader is referred to the web version of this article.)

Table 1

Fitting results for the model with Hg bound to the N atom on thymine's pyrimidine ring.

Parameter	Fitted value
Amplitude	1.93(32)
E_0	−0.12(1.34)
R (N)	2.041(20)
σ^2 (N)	0.00488(303)
R (O)	2.992(44)
σ^2 (O)	0.01137(671)

The R and σ^2 parameters for the C atoms were computed from those for the N atom. R and σ^2 parameters for various multiple scattering paths were computed from these parameters.

(The uncertainties here and in Table 1 represent 1σ statistical variation.) Just slightly more than half of the Hg remains in solution in the sample with 6 mM of Hg, as indicated by the amount of the control spectrum required in the linear combination analysis. From this, we conclude that the DNA is saturated with Hg in the sample with 3 mM Hg and 3 mM duplex DNA.

5. EXAFS analysis

The EXAFS data on the 3 mM Hg+3 mM DNA sample requires an unconventional approach. The linear combination results in Fig. 3 suggest that the Hg is binding directly to the DNA in some manner. (Miyake et al., 2006; Tanaka et al., 2006, 2007) suggest that the Hg binds to the second nitrogen atom on the thymine pyrimidine ring, as shown in Fig. 4. Not knowing *a priori* the nature of the Hg binding, we were forced to consider the possibility of finding the Hg at different locations around each of the four nucleotides. For simplicity of the EXAFS modeling effort, we restricted ourselves to positions of high symmetry. For example, to generate the Hg-containing structure shown in Fig. 4, we assumed that the Hg atom was 2.04 Å from the N atom, equidistant from the neighboring C atoms, and in the plane defined by those three atoms. This was repeated for every pyrimidine, purine, or sugar ring member of each nucleotide. Given atomic coordinates for each such structure, we generated an input file for FEFF, which we then used to generate theory for the EXAFS data analysis. We also considered Hg positions collinear with ligands bound to pyrimidine, purine, or sugar ring members. As one such example, we placed the Hg atom in the line defined by either of the C–O double bonds in thymine's pyrimidine and placed 2.04 Å from the O atom. Again, these configurations were used to generate atomic coordinates for use with FEFF. In total, there were three categories of configurations: (1) Hg bound to a six-member ring, (2) Hg bound to a five-member ring, and (3) Hg bound in a monodentate manner to a ring. These three categories differ in the distance to the second neighbor atom, which, as can be seen by the peak near 2.3 Å in the lower inset to Fig. 2, carries substantial spectral weight in these data.

A cursory examination of these three categories of structural models clearly demonstrates a preference for the first category. Direct binding to a five-member ring and monodentate bonding result in a second coordination shell distance that is inconsistent with the measured data. Any attempt to perform analysis using either of these models resulted in a fit that was of poor statistical quality and that was obviously wrong upon visual inspection. In the remaining discussion, we limit our comments to the situation of an Hg atom bound to a six member ring.

Because of the limited data quality, the information content of these data is quite restricted. Using a Fourier transform range

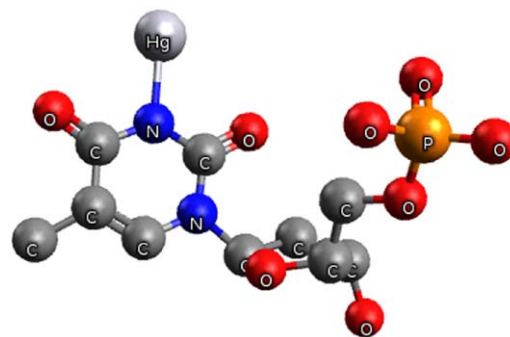


Fig. 4. The thymine nucleotide with a Hg atom bound to the second N atom.

from 2 to 8.8 \AA^{-1} and a fitting range from 1 to 3.1 \AA provides at most 9 independent data points. (Brillouin, 1962) To accommodate this restriction, we made the following parameterizations: (1) the distance from the Hg to the nearest neighbor was one fitting parameter, (2) the ring was assumed to be completely rigid, thus the distance to second neighbor ring members (the C atoms in Fig. 4) was completely determined from the first fitting parameter and trigonometry, (3) the σ^2 for the nearest neighbor was a fitting parameter and the σ^2 for the second neighbor was scaled geometrically by path length from that value, (4) atoms in positions like the two O atoms bound to the pyrimidine ring in Fig. 4 contribute significantly. Their single scattering paths were given ΔR and σ^2 as variables of the fit, and (5) various multiple scattering paths involving the N, C, and O also contribute significant spectral weight and are parameterized in R and σ^2 entirely using the parameters described above and so contribute no new parameters to the fit. Along with E_0 and amplitude parameters, the six variables described in Table 1 were used to make the fit shown in Fig. 5.

Fig. 5 is representative of the quality of fit obtained for any of the fits involving Hg bonded directly to a six-member ring. The Hg atom in the position of Fig. 4 is the slight preference of all possible fits in the six-member ring category, which includes, for instance, Hg bonded to the C atom on the other side of the pyrimidine ring in Fig. 4 and Hg bonded to similar positions on other nucleotides. This slight preference is not, however, of statistical significance.

It is essential that we consider the many assumptions made in this analysis. First, the structural model used in the FEFF calculation may be suspect given that the Hg atom is placed at the periphery of the cluster. That may result in a poorly bounded muffin tin sphere. (Rehr and Albers, 2000) We acknowledge this shortcoming but feel that the short Hg–N bond (to use the example of the structure in Fig. 4) sufficiently constrains the determination of the Hg muffin tin radius by FEFF that the calculation is applicable to our data analysis. Second, the assumption that the Hg atom is in a position of relatively high local symmetry is largely unfounded. However, the severe limitations on the information content of these data require the application of sensible constraints on the parameterization of the fitting model. Third, the assumption that the ring is completely rigid compared to the Hg–N bond is clearly untrue, but the Hg is certainly much more weakly bound to the ring than the ring is to itself. The constraints placed on distances and σ^2 values in the first and second coordination shells are inaccurate, but we assert that they are not so wrong as to invalidate the fitting model.

Acknowledging these limitations to this analysis, we can make several conclusions. First, the EXAFS data are consistent with the Hg atom binding directly to a six-member ring, with a slight preference for the binding being to the N atom in thymine's pyrimidine ring. This is the same conclusion derived from NMR measurements in (Miyake et al., 2006; Tanaka et al., 2006, 2007).

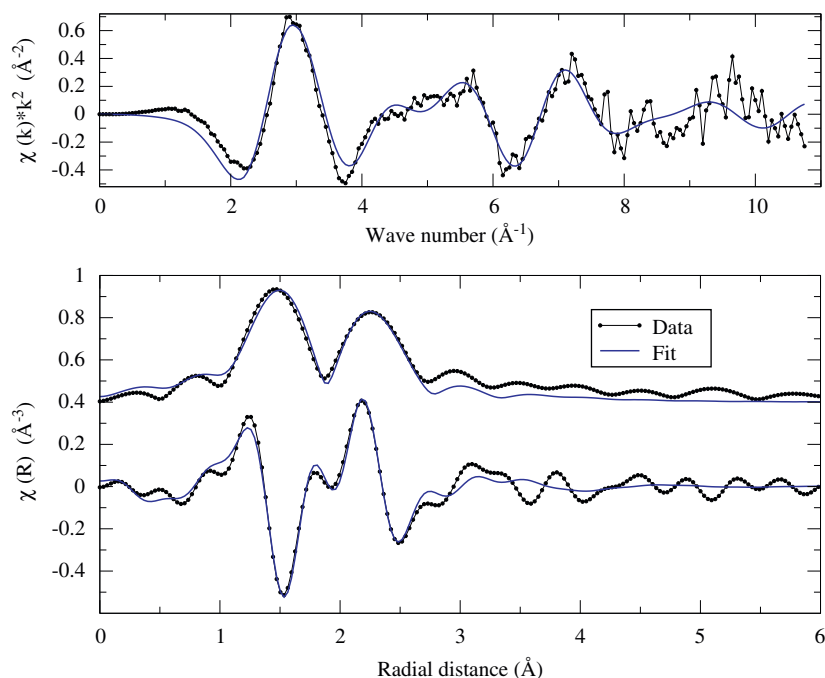


Fig. 5. Results of the fit (blue) in k -space and in R -space to the 3 mM Hg+3 mM duplex DNA data (circles) using the structural model of Fig. 5 and the fitting model described in the text. (For interpretation of the references to colour in this figure legend, the reader is referred to the web version of this article.)

This is a sensible location for the Hg atom. The hydrogen bond linking a thymine to its usual Watson–Crick pair, adenine, is through that N atom. However, the hydrogen bond is unable to form in the DNA duplex used here because of the thymine–thymine mispairing, and thus the N atom may bind to Hg in lieu of forming a true Watson–Crick bond. Second, the fitted values of all the parameters are reasonable. The Hg–N distance is approximately the same as the short Hg–O distances in inorganic HgO (Aurivillius, 1964), so is quite reasonable for the bond between Hg and a first row element. The other parameters are also defensible, although the σ^2 values are rather large for this low temperature, suggesting that the real sample possesses more disorder about the Hg than in the highly symmetric structural model of Fig. 4.

That the amplitude term is close to 2 merits attention. Using a value for S_0^2 obtained from analysis of inorganic HgO (not shown) of 0.82(6), this yields a coordination number of $N_c = 2.36(43)$. In (Miyake et al., 2006; Tanaka et al., 2006, 2007), the authors posit that the binding site for the Hg is between a thymine–thymine mismatch in this duplex DNA. As stated above, our data only allow us to assert that the Hg is in some position binding to a six-member ring without definitively identifying which one. That it bridges a thymine–thymine mismatch is certainly consistent with our results.

6. Conclusions

We have made EXAFS measurements on Hg in catalytic-DNA-based sensor systems. We find a strong affinity to a single binding site on the Hg-selective DNA. This result is consistent with the transient 1:1 binding species found by the NMR results of Miyake et al. (2006). Analysis of the Hg-edge EXAFS shows that the Hg is bound directly to a six-member ring, although our data are not of sufficient quality to definitively identify which such position among the four nucleotides is the binding site. The assertion in (Miyake et al., 2006; Tanaka et al., 2006, 2007) that the Hg bridges two

thymines is consistent with our results. In this work we have outlined an unconventional analytical approach using the popular software tools, FEFF and IFEFFIT.

This class of DNA-based sensors can be adapted for a wide variety of metal contaminants. New EXAFS measurements are under way on sensors for aqueous lead and copper as well as for soluble dioxo-uranyl compounds.

As a final statement, we remind the reader that the EXAFS measurement is sensitive only to the local structure around the absorbing atom. A full and detailed understanding of the DNA/metal interaction would require knowledge of the mesoscopic structure, such as how the entire DNA molecule restructures itself in the presence or absence of the metal. Questions of mesoscopic structure are beyond the capacity of an EXAFS measurement. Still, the atomistic understanding of the interaction of the metal with its ligand is certainly an important part of the story.

Acknowledgements

Ying He's key assistance in the preparation of this manuscript is gratefully acknowledged. This work was supported in part by the US Department of Energy, Office of Science, under Contract no. DE-FG02-08ER64568 and the NSF WaterCAMPWS Science and Technology Center (CTS-0120978). Use of the Advanced Photon Source was supported by the US Department of Energy, Office of Science, Office of Basic Energy Sciences, under Contract no. DE-AC02-06CH11357. PNC/XOR facilities at the Advanced Photon Source, and research at these facilities, are supported by the US Department of Energy—Basic Energy Sciences, a major facilities access grant from the NSERC, the University of Washington, Simon Fraser University and the Advanced Photon Source. Use of the Advanced Photon Source is also supported by the US Department of Energy, Office of Science, Office of Basic Energy Sciences, under Contract no. DE-AC02-06CH11357.

References

- Aurivillius, K., 1964. Least-squares refinement of the crystal structures of orthorhombic HgO and of Hg₂O₂NaI. *Acta Chem. Scand.* 18 (5), 1305–1306.
- Brillouin, L., 1962. *Science and Information Theory*. Academic Press, New York.
- Li, J., Lu, Y., 2000. A highly sensitive and selective catalytic DNA biosensor for lead ions. *J. Am. Chem. Soc.* 122, 10466–10467.
- Liu, J., Lu, Y., 2007. Rational design of “Turn-on” allosteric DNAzyme catalytic beacons for aqueous mercury ions with ultrahigh sensitivity and selectivity. *Angew. Chemie (Int. ed. Engl.)* 46, 7587–7590.
- Liu, J., Brown, A.K., Xiangli, M., Cropek, D.M., Istok, J.D., Watson, D.B., Yi, L.U., 2007. A catalytic beacon sensor for uranium with parts-per-trillion sensitivity and millionfold selectivity. *Proc. Natl. Acad. Sci.* 104 (7), 2056–2061.
- Miyake, Y., Togashi, H., Tashiro, M., Yamaguchi, H., Oda, S., Kudo, M., Tanaka, Y., Kondo, Y., Sawa, R., Fujimoto, T., Machinami, T., Ono, A., 2006. Mercury^{II}-mediated formation of thymine–Hg^{II}–thymine base pairs in DNA duplexes. *J. Am. Chem. Soc.* 128, 2172–2173.
- Newville, M., 2001. IFEFFIT: interactive XAFS analysis and FEFF fitting. *J. Synchrotr. Radiat.* 8, 322–324.
- Ravel, B., Newville, M., 2005. ATHENA, ARTEMIS, HEPHAESTUS: data analysis for X-ray absorption spectroscopy using IFEFFIT. *J. Synchrotr. Radiat.* 12, 537–541.
- Ravel, B., 2008. <<http://cars9.uchicago.edu/iffwiki/Demeter>>.
- Rehr, J.J., Albers, R.C., 2000. Theoretical approaches to X-ray absorption fine structure. *Rev. Mod. Phys.* 72 (3), 621–654.
- Tanaka, Y., Yamaguchi, H., Oda, S., Kondo, Y., Nomura, M., Kojima, C., Ono, A., 2006. NMR spectroscopic study of a DNA duplex with mercury-mediated T–T base pairs. *Nucleos. Nucleot. Nucleic Acids* 25, 613–624.
- Tanaka, Y., Oda, S., Yamaguchi, H., Kondo, Y., Kojima, C., Ono, A., 2007. ¹⁵N–¹⁵N J-Coupling Across Hg^{II}: direct observation of Hg^{II}-mediated T–T base pairs in a DNA duplex. *J. Am. Chem. Soc.* 129, 244–245.